

Chapter 8

Numerical modelling of building response to tunnelling: Example analyses

8.1 Introduction

This Chapter describes examples of three-dimensional numerical analysis of building response to tunnelling. The analyses are used to evaluate the use of beam elements for modelling masonry building facades in 3D during finite element tunnelling simulations, using the developments described in the previous Chapters of this thesis. The analyses allow an evaluation of the 3D beam approach for modelling masonry buildings and the equivalent elastic and equivalent masonry beam models for assigning properties to the beams. This evaluation is by comparison with finite element analyses, based on previous work at Oxford University, containing full finite element models of the buildings. (Evaluation of the 3D beam approach with respect to tunnelling case histories is undertaken in Chapter 9). Two different problems are analysed: a symmetric problem where the tunnel passes square under the centre of a masonry building, and an oblique problem where the building is both eccentric to the tunnel centre line and skewed at an angle. Results are presented for

a number of finite element analyses of both the symmetric and oblique problems. Surface displacements and building damage predictions resulting from the finite element analyses using surface beam elements to represent the building, finite element analyses using full building facades and traditional hand assessments are compared.

8.2 Symmetric analysis

8.2.1 Description of analysis

The first example problem consists of a tunnel constructed with the centre line passing symmetrically beneath the middle of a rectangular building which is aligned with its front and rear facades perpendicular to the direction of tunnelling as shown in figure 8.1. The example problem is identical to that used by Augarde (1997), Liu (1997), Burd et al. (2000) and Wisser (2002) during their development of numerical methods for modelling tunnel construction, masonry facades and compensation grouting. Four different finite element analysis run types are undertaken with the symmetric problem as summarised in table 8.1: the first type (SGF) is a greenfield analysis with no building present; the second (SMF) includes a full masonry building on the surface made from 2D facades; thirdly, surface beams with properties determined using the equivalent elastic beam method are used to represent the building (SEB); and finally the building is represented by surface beams using the equivalent masonry beam model (SMB). The SGF and SMF analyses are repeats of the previous Oxford University work, but this is necessary so that comparisons with the surface beam analyses are not mesh dependent.

Table 8.1: **Description of finite element run types for symmetric analyses**

FE Runs	Description of Analysis
SGF	Symmetric Greenfield
SMF	Symmetric with building made of 2D Masonry Facades
SEB	Symmetric with Equivalent Elastic Beams representing the building
SMB	Symmetric with Equivalent Masonry Beams representing the building

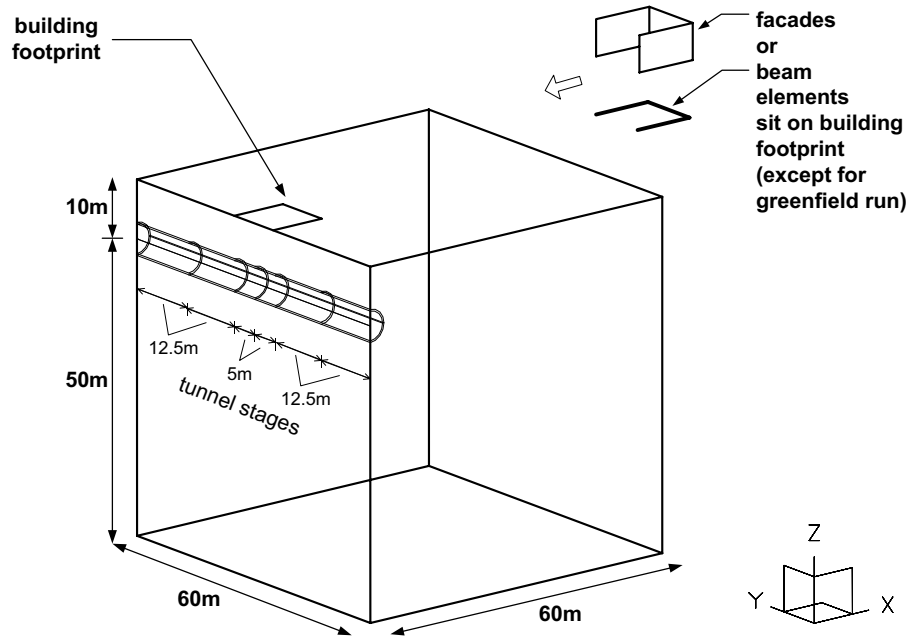


Figure 8.1: Symmetric example analysis layout

Geometry and mesh

The layout of the symmetric example problem is shown in figure 8.1. It consists of a tunnel of 5m inner diameter constructed at a centreline depth of 10m. On the surface is a building 20m long, 10m wide and 8m high. The building comprises 1m thick masonry walls and has windows and a door in the front and rear facades (which are identical) with dimensions as shown in figure 8.2. The end walls of the building are plain with no openings.

The tunnel lining is 0.25m thick concrete making the outer diameter of the tunnel 5.5m. Volume loss applied to the tunnel is 2%. Due to symmetry, only half the problem is analysed using a soil block with dimensions of 60m in all three directions.

The soil mesh for all the symmetric analyses is shown in figure 8.3 with the building mesh for run type SMF and the beam mesh for run types SEB and SMB shown in figure 8.4. The soil and tunnel mesh contains 9993 nodes and 6558 ten-noded tetrahedral elements. The building mesh for run type SMF has 1562 nodes and 679 six-noded triangular plane stress elements; and for run types SEB and SMB, the surface beams comprise 64 Timoshenko beam elements. The surface beam nodes are selected to match nodes on the building footprint of the soil mesh (which also correspond to nodes at the base of the facade mesh).

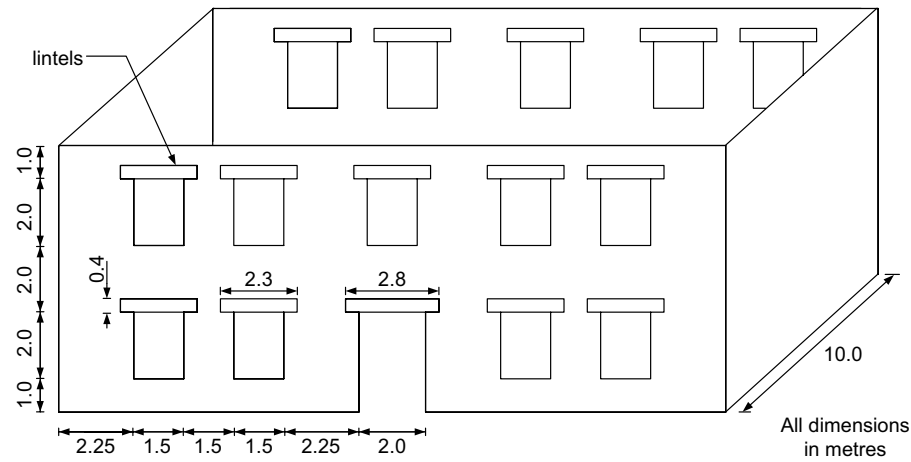


Figure 8.2: **Building for example analyses**

The boundary conditions applied to the soil are: fully fixed displacements (x , y and z displacements fixed) at the base; and horizontal displacements (x or y displacements as appropriate) fixed perpendicular to each vertical soil boundary. For run SMF the 2D plane stress elements in the building mesh have fixed horizontal (x displacement fixed) displacement at the plane of symmetry. For run types SEB and SMB the surface beams have fixed horizontal displacements (x displacement fixed) and fixed rotation about the y -axis at the plane of symmetry.

Soil and tunnel properties

The soil is modelled using the nested yield surface model described in section 7.4. The properties for the model are given in table 8.2 and are identical to those chosen to represent London Clay in previous analyses at Oxford University (for example Augarde, 1997 and Wisser, 2002). The soil is assumed to have a ratio of horizontal to vertical stress of 1.125. The elastic properties for the concrete tunnel lining are given in table 7.1.

Building and beam properties

For run type SMF, the building facades are assigned the no-tension masonry material model developed by Liu (1997) with the properties described in section 5.3 and given in

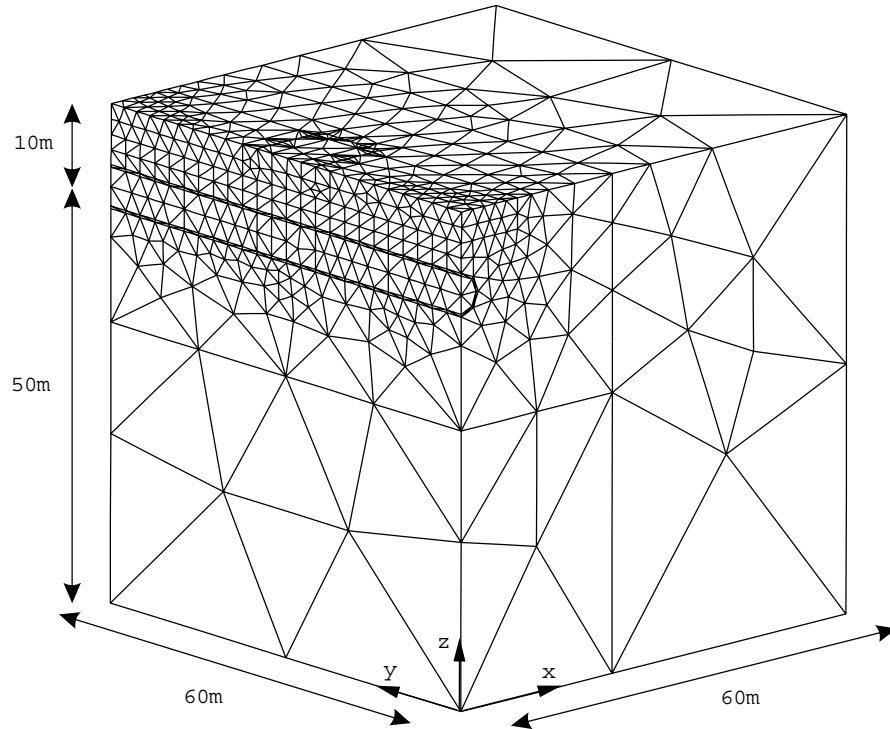
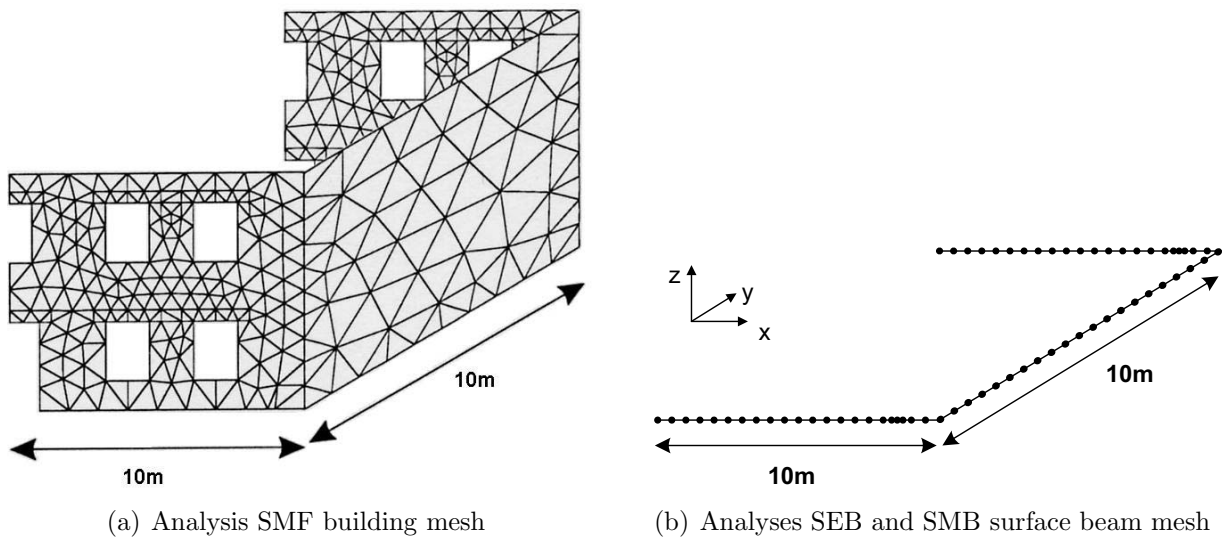


Figure 8.3: Symmetric example analysis soil mesh



(a) Analysis SMF building mesh

(b) Analyses SEB and SMB surface beam mesh

Figure 8.4: Symmetric example analyses building meshes

Table 8.2: Material properties for nested yield surface soil model

G_0^s	s_{u0}	ω	μ	γ	ν
$3.0 \times 10^4 \text{kPa}$	60.0kPa	$3.0 \times 10^3 \text{kPa/m}$	6.0kPa/m	20kN/m ³	0.49
<i>Surface</i>		c'_α	g'_α		
1		0.020	0.900		
2		0.040	0.750		
3		0.060	0.500		
4		0.100	0.300		
5		0.150	0.200		
6		0.200	0.150		
7		0.300	0.100		
8		0.500	0.050		
9		0.700	0.025		

table 5.2. Elastic lintels above the windows are also included (as shown in figure 8.2) with the properties given in table 5.3.

For runs SEB and SMB, the surface beams are assigned properties using the equivalent elastic and equivalent masonry beam methods as described in Chapters 4 and 5 respectively. Properties denoted as *in-plane* and *out-of-plane* refer to the planes of the 2D facade that the beams represent, where out-of-plane properties are those associated with displacements perpendicular to the plane of the facade. On application of those methods to the facades shown in figure 8.2, the effective cross sectional area, A^* , and the effective second moment of area in-plane, I^* , are calculated for both the front/rear facade and the end walls. For this building the base conditions are assumed to be smooth for the calculation of the beam properties. Appendix C contains an example of the full calculation of the properties for the beams to represent the front and rear facades, the results of which are given in table 8.3. Table 8.4 contains the properties for the beams representing the end wall. In tables 8.3 and 8.4: E is Young's modulus, G is the shear modulus, J is the torsional rigidity, k is the shear coefficient and γ is the self weight. All properties are the same for the equivalent elastic beams (EEB) and the equivalent masonry beams (EMB) with the exception of the critical curvature (κ_{crit}) and residual in plane bending factor (f_b) which are not applicable for the EEBs. Parametric studies of the effect of assigning different properties from those described in this section for the EEBs and EMBs are investigated in sections 8.2.4 and

Table 8.3: **Material properties for surface beams: Front/rear building facade**

E	G	A^*	I_{in}^*	I_{out}^*
$1.00 \times 10^7 \text{kPa}$	$4.167 \times 10^6 \text{kPa}$	4.762m^2	29.716m^4	0.397m^4
J	k	γ	κ_{crit} (EMB only)	f_b (EMB only)
1.353m^4	0.85	20.0kN/m^3	1.0×10^{-5}	0.01

Table 8.4: **Material properties for surface beams: End wall**

E	G	A^*	I_{in}^*	I_{out}^*
$1.00 \times 10^7 \text{kPa}$	$4.167 \times 10^6 \text{kPa}$	3.333m^2	17.778m^4	0.278m^4
J	k	γ	κ_{crit} (EMB only)	f_b (EMB only)
0.921m^4	0.85	20.0kN/m^3	1.0×10^{-5}	0.01

8.2.5 below.

The walls are assumed to have a self weight of 20kN/m^3 . Self weight is applied to the facades for run SMF while for the surface beams, loads are calculated using the facade dimensions described above and are applied at the nodal points on the surface beams. The loads differ from node to node due to the openings in the facades.

Calculation procedure

The finite element calculation proceeds in stages to simulate the stress history at the site and progressive construction of the tunnel as described in section 7.3. Table 8.5 shows the stages used for the symmetric analyses. In the first calculation stage, the building self weight and soil initial stresses are applied. In the second stage the building strains and displacements are reset to zero. This ensures that the strains, building damage and surface displacements recorded during subsequent tunnelling are due the construction of the tunnel alone. The tunnel is then constructed in six stages; the length of each stage in the y -direction varies and is given in table 8.5.

There are two exceptions to the general procedures. Firstly, for run type SMF with the building represented by masonry facades, the masonry material residual tensile strength, c is initially set to 0.0kPa while the building self weight is applied to the model (stages 1 and 2 from table 8.5). The residual tensile strength is then changed to 10kPa at the

Table 8.5: Calculation stages for symmetric example analysis

Stage	No. Steps	Description
1	15	Application of building weight and initial soil stresses
2	10	Reset displacements and strains to zero
3	15 (30 for SMB)	Tunnel construction stage 1: 00.0 - 12.5m
4	15 (30 for SMB)	Tunnel construction stage 2: 12.5 - 25.0m
5	15 (30 for SMB)	Tunnel construction stage 3: 25.0 - 30.0m
6	15 (30 for SMB)	Tunnel construction stage 4: 30.0 - 35.0m
7	15 (30 for SMB)	Tunnel construction stage 5: 35.0 - 47.5m
8	15 (30 for SMB)	Tunnel construction stage 6: 47.5 - 60.0m

commencement of tunnelling (stage 3). This approach was used by Wisser (2002) to avoid any tensile stress accumulating in the facades during the self weight loading contributing to the cracking of the building in the later tunnelling stages. It is adopted here as this approach is thought to provide more realistic facade response predictions to the tunnelling.

Secondly, for the run type SMB, the accumulation of stress in the first two stages also needs to be avoided in order to allow for assessment of displacements simply due to tunnelling. For SMB runs, this is achieved by simply adding the masonry beam elements only after stage 2 is complete.

The number of calculation steps per stage is chosen as 15 steps for all analyses except the SMB analyses where the number of steps is chosen as 30 in order to reduce the out-of-balance forces generated during the calculation procedures to acceptable levels. The choice of the number of steps per stage is based on recommendations presented by Wisser (2002) who investigated differing numbers of steps and corresponding out-of-balance forces.

8.2.2 Greenfield analysis

This section details the results of the symmetric greenfield run SGF, with no building on the surface. The purpose of this run is to provide greenfield surface settlement results to act as a control for the later runs which include the building on the surface.

Figure 8.5 shows the surface contours after each tunnelling stage while figure 8.6 shows the surface profile development in 3D. The colours in the 3D plots match the colour key in the

relevant contour plots, but the surface grid shown is unrelated to the finite element mesh. This applies for all the contour and 3D plots presented in the remainder of this thesis.

Also throughout this thesis, the direction of tunnelling is referred to as the *longitudinal* direction while the direction perpendicular to the tunnel is called the *transverse* direction. Vertical surface displacements are shown in figure 8.7 along transverse lines at $y=25\text{m}$ (a) and $y=35\text{m}$ (b); along the longitudinal centre line of the tunnel (c); and along a longitudinal line under the end wall of the building $x=10\text{m}$ (d), for each tunnelling stage 1-6.

Charts 8.5 to 8.7 show a smooth greenfield surface profile developing as the tunnel progresses. The greenfield surface displacement results, however, show a transverse settlement trough that is wider and shallower than the semi-empirical Gaussian curve commonly attributed to greenfield settlements as discussed in section 2.2. The semi-empirical curve for this example problem is shown along with the transverse finite element settlements in figure 8.8. A greenfield trough that is shallower and wider than the Gaussian approximation is a common feature of finite element analyses as discussed in sections 2.3.2 and 2.4. This feature does not limit the usefulness of the SGF run for use as a control for the comparison with runs with buildings on the surface. The longitudinal trough displays steady state settlement approximately 15m behind the tunnel face, a distance of five tunnel diameters.

Model SGF thus provides a greenfield reference base against which the influence of including a building on the surface, by means of facades (SMF run), or surface beams (SEB and SMB runs), is compared in the remainder of the symmetric analyses described below.

8.2.3 Analysis with masonry building

Surface displacement results from run type SMF with the building comprising 2D masonry facades are presented in figures 8.9 to 8.11.

The influence of the building on the settlement profile is clearly observable as comprising two main effects. The first is the influence of the building weight adding to the magnitude of the displacement under all the building facades. This is particularly evident in the 3D

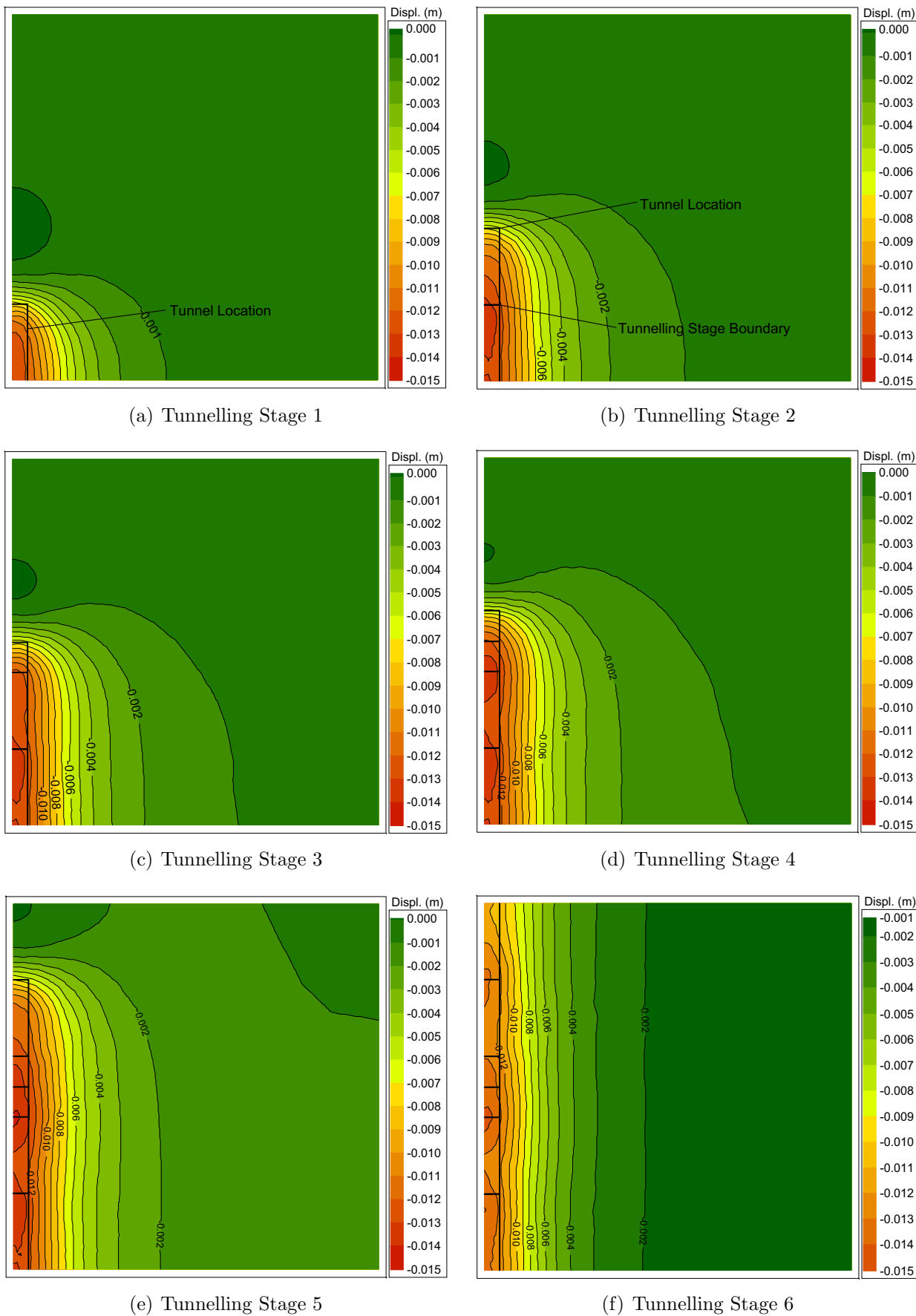
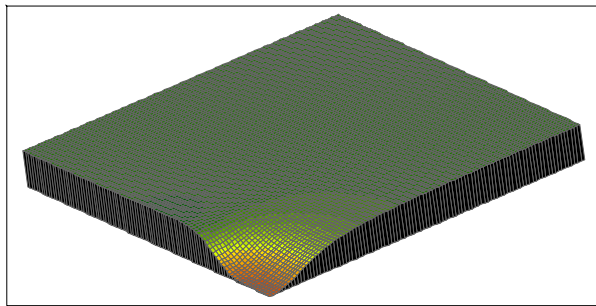
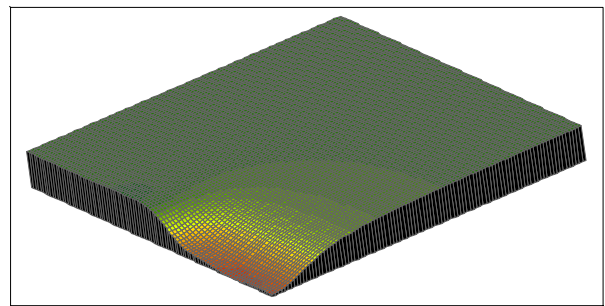


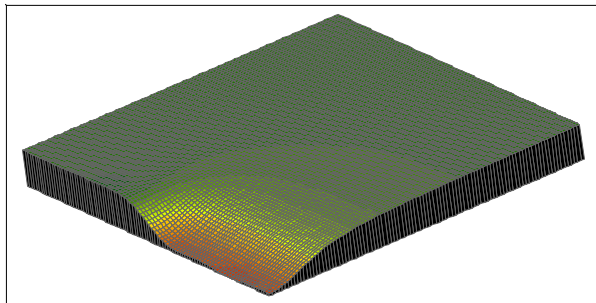
Figure 8.5: Greenfield run SGF: Surface displacement contours



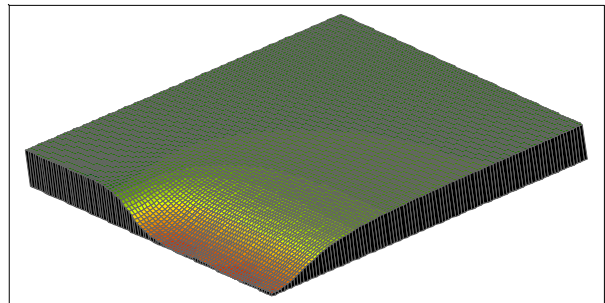
(a) Tunnelling Stage 1



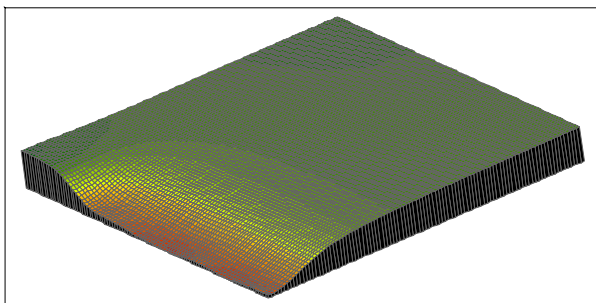
(b) Tunnelling Stage 2



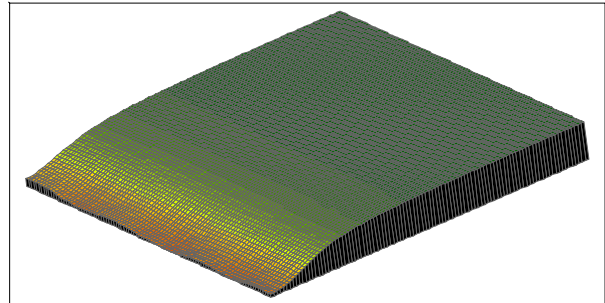
(c) Tunnelling Stage 3



(d) Tunnelling Stage 4

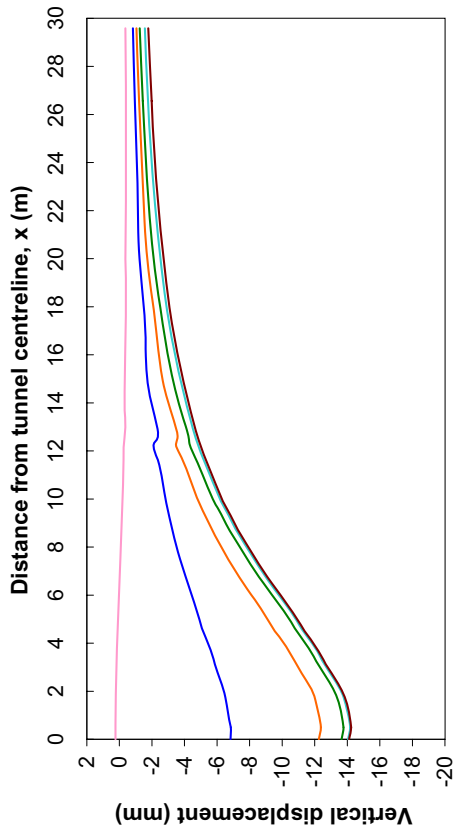


(e) Tunnelling Stage 5

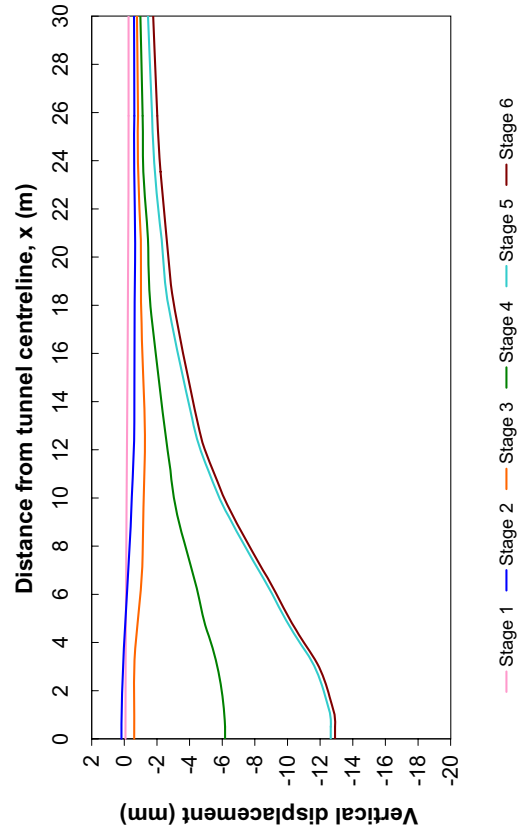


(f) Tunnelling Stage 6

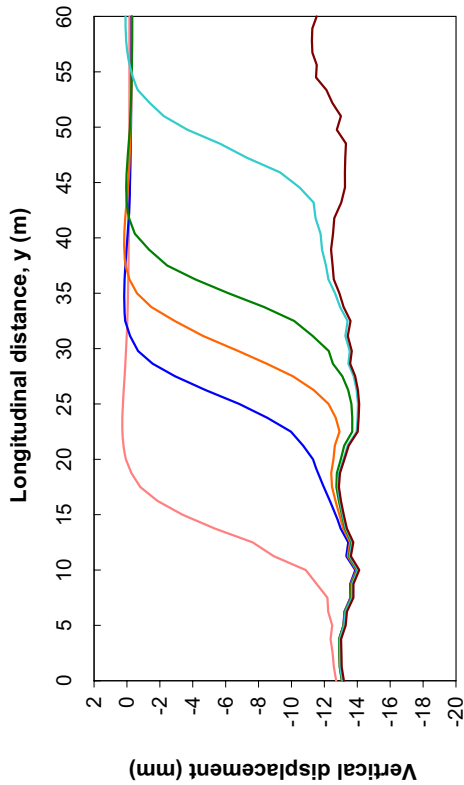
Figure 8.6: Greenfield run SGF: 3D Surface profile



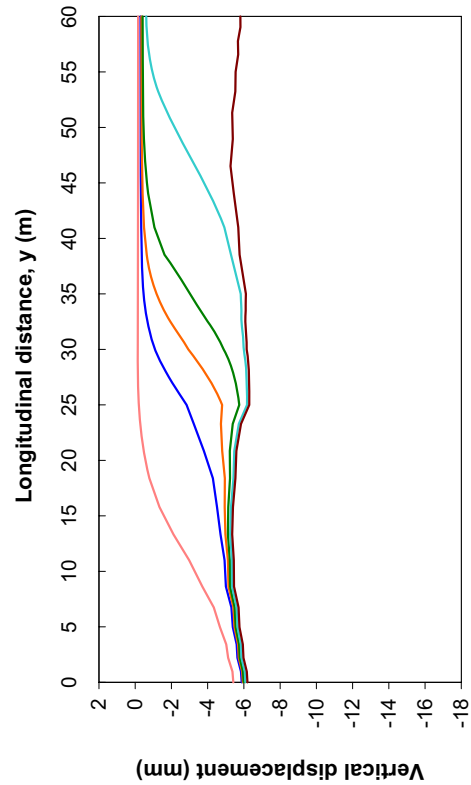
(a) Transverse $y=25\text{m}$



(b) Transverse $y=35\text{m}$



(c) Longitudinal tunnel centre line $x=0\text{m}$



(d) Longitudinal end wall $x=10\text{m}$

Figure 8.7: Greenfield run SGF: Surface displacements

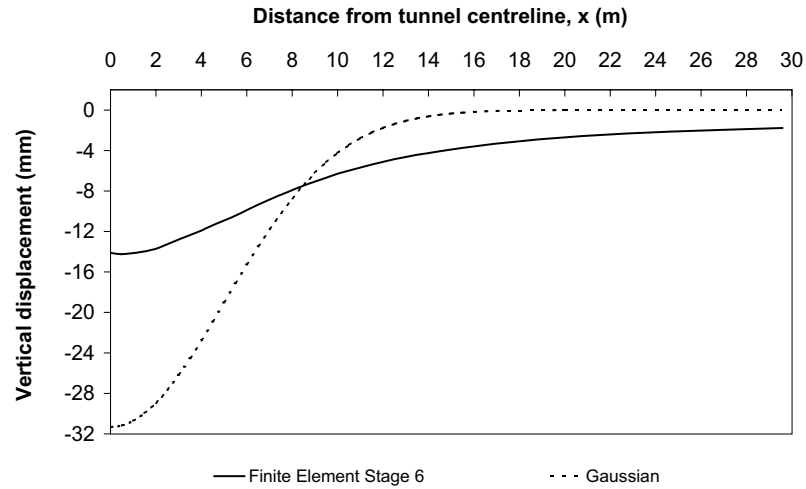


Figure 8.8: **Greenfield run SGF: Comparison with transverse Gaussian Settlement ($y=25\text{m}$)**

plots and the longitudinal centre line and $x=10\text{m}$ plots in figure 8.11 when comparing these to the corresponding greenfield plots in figure 8.7.

Secondly, the transverse surface profile is flattened by the presence of the building. In this analysis the building lies almost completely in a sagging zone of displacement. It is expected, therefore, that the masonry building will respond in a rigid manner with little sagging curvature; a response which is clearly evident in the SMF results. As described in section 5.2, this rigid response with a flat displacement profile, is due to arching effects within the masonry facades (Liu, 1997) acting to flatten the curvature of the surface settlements in sagging. These observations concur with those of Burd et al. (2000) in connection with an analysis of the same problem.

It is interesting to note that as the tunnelling progresses the front and rear facades settle in a rigid fashion with no tilt and minimal curvature. The end wall, while remaining in a very slight hogging state, could also to be considered to act rigidly as the tunnelling progresses. Following the final stage of tunnelling, it can be seen that the building remains tilted, with the front facade approximately 1.5mm lower than the rear. This is also evident from the end wall plot for tunnelling stage 6 (figure 8.11(d)).

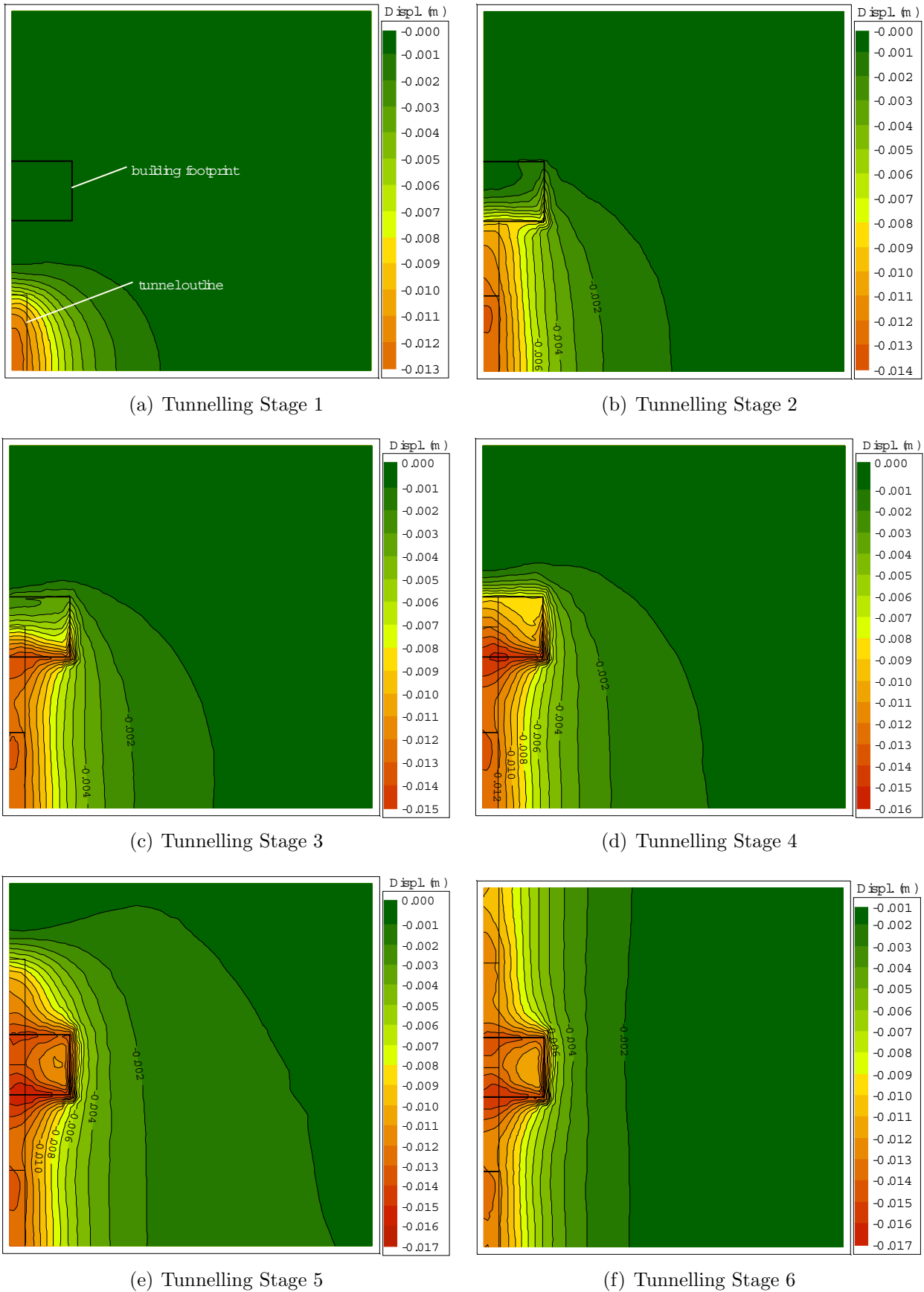
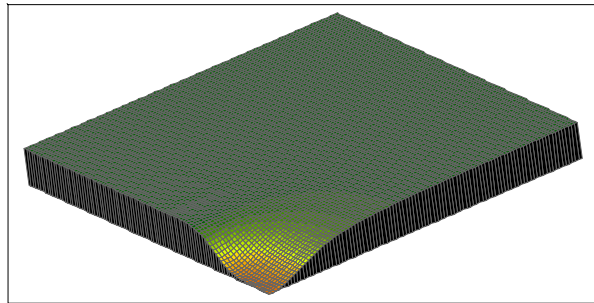
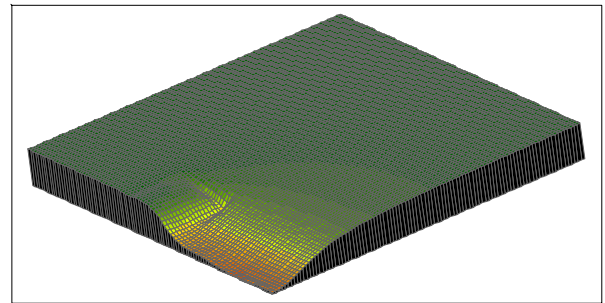


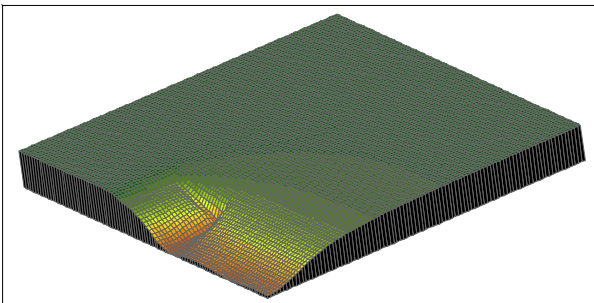
Figure 8.9: Masonry building run SMF: Surface displacement contours



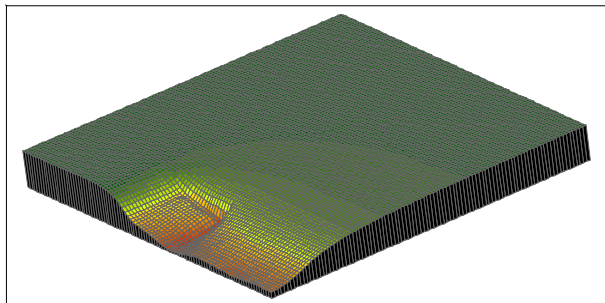
(a) Tunnelling Stage 1



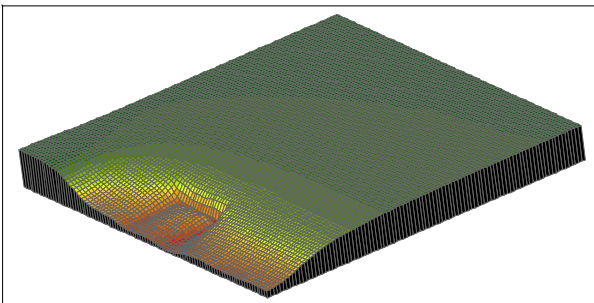
(b) Tunnelling Stage 2



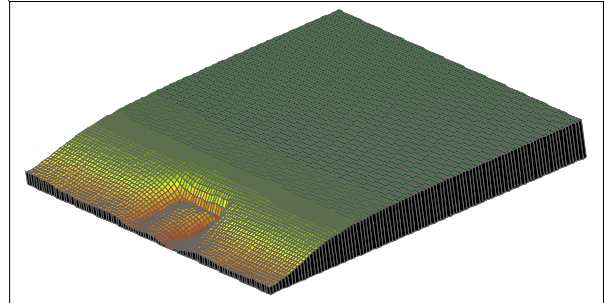
(c) Tunnelling Stage 3



(d) Tunnelling Stage 4



(e) Tunnelling Stage 5



(f) Tunnelling Stage 6

Figure 8.10: Masonry building run SMF: 3D Surface profile

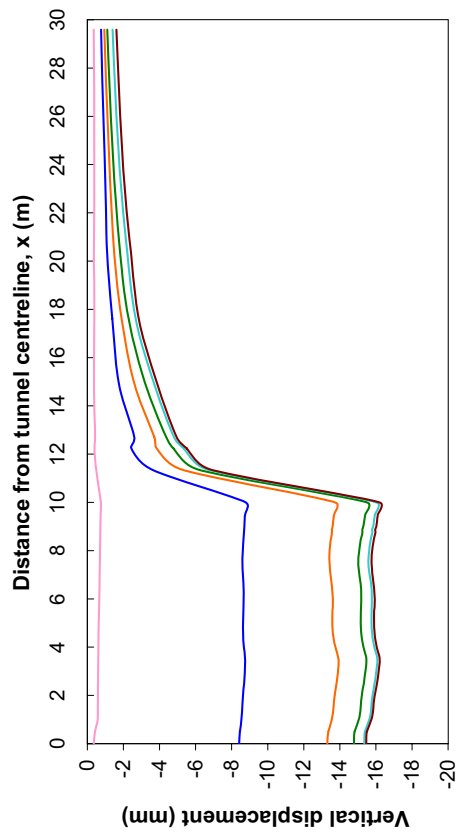
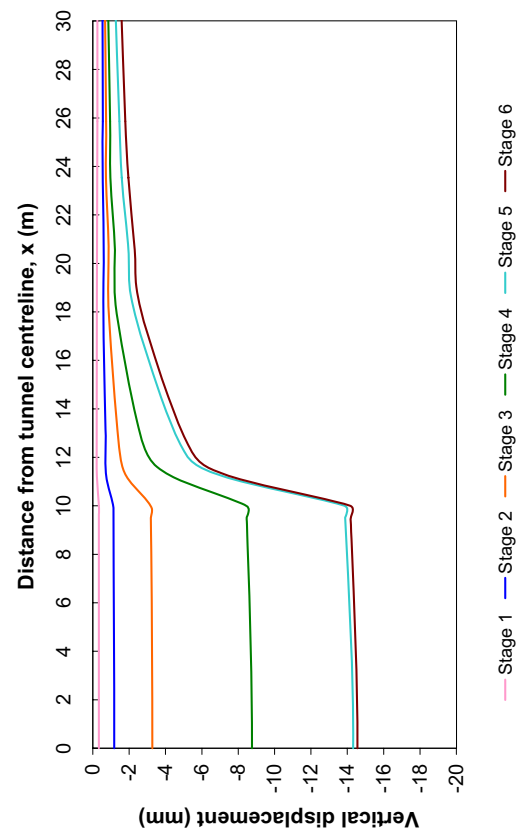
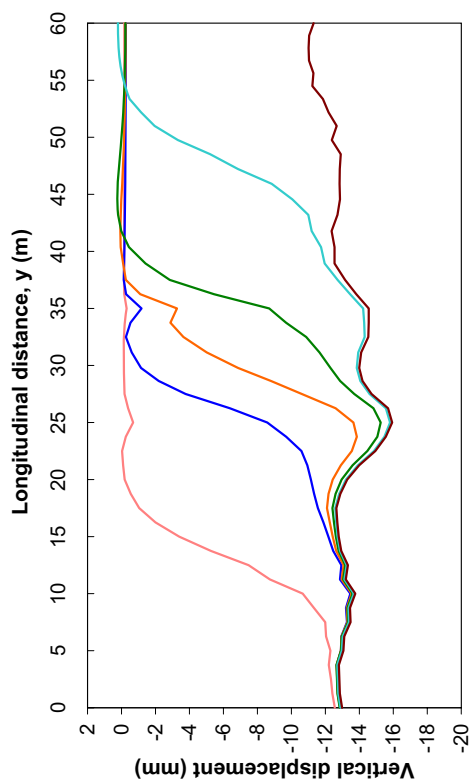
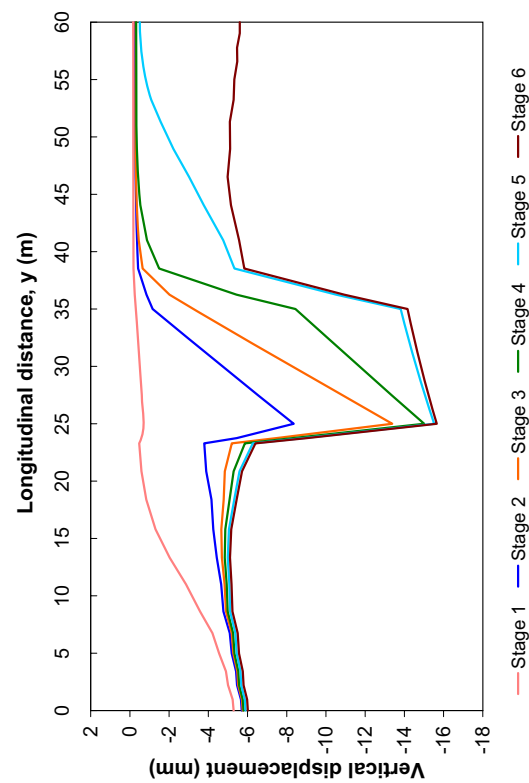
(a) Transverse $y=25\text{m}$ (b) Transverse $y=35\text{m}$ (c) Longitudinal tunnel centre line $x=0\text{m}$ (d) Longitudinal end wall $x=10\text{m}$

Figure 8.11: Masonry building run SMF: Surface displacements